Nonlinear Laser Fluorescence Spectroscopy of Natural Organic Compounds

30

Victor V. Fadeev and Evgeny A. Shirshin

Contents

Abstract

Principles of nonlinear laser fluorescence spectroscopy of complicated organic compounds and of the method capable of determining photophysical parameters are considered in this chapter. Special attention is paid to the peculiarities of the method connected with specific photophysical processes in natural organic

V.V. Fadeev (✉) • E.A. Shirshin
Moscow State University, Moscow, Russian Federation
e-mail: victor_fadeev@mail.ru, eshirshin@gmail.com

V.V. Tuchin (ed.), *Handbook of Coherent-Domain Optical Methods*,

DOI 10.1007/978-1-4614-5176-1_30,

compounds, especially in proteins, and to the major role of intramolecular energy transfer and presence of localized donor-acceptor pairs (LDAP) of fluorophores within single macromolecules. These facts stimulated the development of models based on the collective states formalism describing fluorescent response of LDAP to pulsed laser excitation. Unique features of the method are illustrated by the example of proteins (proteins with intrinsic fluorescence (HSA, BSA) and fluorescent protein mRFP1) that can be used as fluorescent tags of intracellular processes while their photophysical parameters can be used as the information channel.

30.1 Introduction

The use of lasers (laser radiation) has dramatically changed optics and optical spectroscopy [1–3]. Many of the traditional methods of spectroscopy had a rebirth, the most striking examples being spectroscopy of spontaneous Raman scattering [2, 4], opto-kalorimetric methods (the method of termolens, optoacoustic spectroscopy, etc.) [2, 3]. Of greater scientific interest and practical importance are the "true laser" techniques, based on the nonlinearity and coherent optical response of the medium on laser radiation. For example, these methods include intracavity laser spectroscopy [3], laser spectroscopy within the Doppler line [2], coherent anti-Stokes Raman spectroscopy (CARS) [2], nonlinear spectroscopy of surface (SERS, the second and the third harmonic spectroscopy [1]), and parametric scattering of light spectroscopy [1, 2, 5].

For a long time, the method of fluorescence spectroscopy stood apart from this process, though this method has high sensitivity [6]. The principal limitations of classical fluorometry are its low selectivity caused by broad and unstructured fluorescence emission bands and the fact that this method is very limited at the solution of the inverse problem (i.e., at determination of photophysical characteristics of fluorescent molecules). In the early 1970s, the prospects of using fluorescence in remote laser (lidar) sensing of the atmosphere and, especially, the hydrosphere were demonstrated [7], and extensive application of laser diagnostics in medicine and biology [8] became incentives for seeking ways of making fluorometry more informative.

These studies led to the creation of the method of nonlinear laser fluorescence spectroscopy [9–11]. In this method, fluorescence saturation curves (nonlinear dependencies of fluorescence intensity on the exciting radiation) are used as the input data for solving of the inverse problem. In the framework of solving just one inverse problem, using a single saturation curve measured on a single spectrometer, one can simultaneously determine the photophysical characteristics (absorption cross section, the lifetime of the excited state, the rates of energy transfer, etc.), measuring which in classical spectroscopy would require the use of different tools and techniques, and, moreover, it can be done without a priori information required for classical methods, such as the concentration of molecules (for determining the absorption cross section), the lifetime of the excited state of the donor in the absence of the acceptor (for determining the rate of energy transfer), and so on.

Laser fluorometry turned out to be a unique method of studying natural organic compounds, photosynthetic organisms [12], proteins [13–15] (especially fluorescent proteins [14, 15]), and humic substances [16], which, moreover, can be used as fluorescent descriptors and indicators of the ecosystem state to which they belong. An important property of the majority of natural complex organic compounds (COC) in scope of optical spectroscopy is a high local concentration of absorbing (chromophores) and fluorescing (fluorophores) groups located within a single macromolecule, while the concentrations of these macromolecules in media are usually low. This fact predetermines a major role of intramolecular energy transfer. Some of the natural COC typically have a determined countable number of chromophores/fluorophores with a possible energy transfer between them (e.g., localized donor-acceptor pairs [14]). All these require the development of novel methods based on the laser fluorescence spectroscopy technique.

This chapter outlines the basis of nonlinear laser fluorescence spectroscopy of complex organic compounds. The possibilities of laser fluorometry are illustrated by the results of its application in the research and diagnostics of extremely important natural organic compounds - proteins, including fluorescent proteins that are of great interest as indicators of living cells' state. The choice of these objects has been determined both by their importance in nature and the variety of photophysical processes that allows illustration of unique possibilities of nonlinear laser fluorometry.

In this chapter, human and bovine serum albumins (HSA and BSA [13, 14]) and red fluorescent protein mRFP1 [14, 15] are represented. The complexity of photophysical processes in this sequence increases and requires the development of the analysis method.

30.2 Fundamentals of Nonlinear Laser Fluorescence Spectroscopy of Complex Organic Compounds (COC)

30.2.1 Photophysical Processes in COC. Photophysical Parameters

Both classical (linear) and laser fluorescence spectroscopy of complex organic compounds (COC) are based on the phenomenon of fluorescence. The model of fluorescence response formation under optical excitation operates with a set of photophysical parameters – the absorption (or excitation) cross section, fluorescence quantum yield, the rates of radiative and non-radiative excited state relaxation, the rate of singlet-triplet conversion, and the rate of intermolecular energy transfer, including energy transfer between similar molecules in the excited state (singlet-singlet annihilation). The processes and capabilities of classical fluorescence spectroscopy (fluorometry) are presented in many monographs (see, e.g., [6]). The information below is provided to present the foundations of nonlinear laser fluorometry.

Fluorescence, or fast luminescence, is the result of the allowed radiative transitions from the excited electronic state to the ground one. The diagram of the lowest

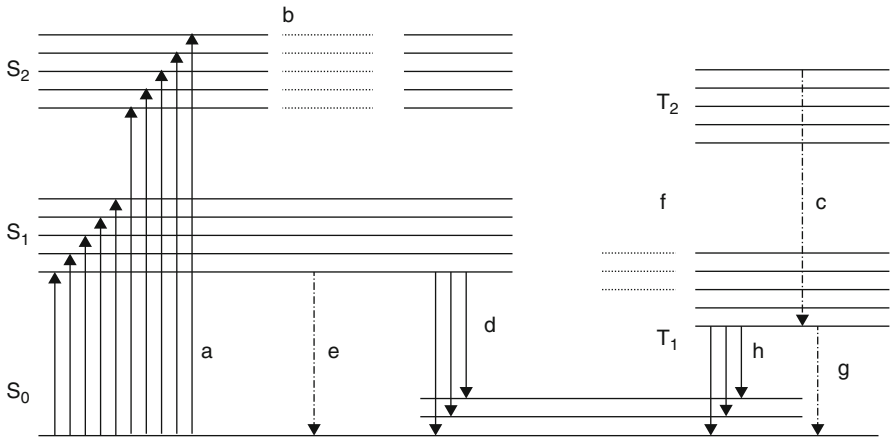

Fig. 30.1 Lowest energy levels of COC molecule and possible photophysical processes: *a* – absorption; *b* – internal conversion; *c*, *e*, *g* – nonradiative decay; *d* – fluorescence emission; *f* – singlet-triplet conversion; *h* – phosphorescence

molecules' energy levels is presented on Fig. 30.1. For the majority of molecules with an even number of electrons in ground state, all the molecular orbitals (MO) are filled with pairs of electrons (i.e., the orbital contains an even number of electrons).

According to the Pauli exclusion principle, electrons of the same MO have opposite spins, hence, the resultant spin quantum number (S) for the molecules in the ground state is zero ($S = 0$) and the multiplicity $J = |2S + 1| = 1$. However, when one electron goes to the upper orbital, its spin can be oriented in either the same or the opposite direction to that of the remainder of the lower orbital electron. In the first case, $S = 0, J = 1$, and the excited state is singlet; in the second, $S = 1, J = 3$, and the state of the molecule is triplet.

Each electronic level of an organic molecule splits into a series of vibrational levels, and each vibrational level into a series of closely spaced rotational sublevels. Collision of molecules and electrostatic perturbation induced by the surrounding solvent molecules leads to broadening of the vibrational-rotational sublevels. As a result, a quasicontinuum of energy states appears. Therefore, absorption and fluorescence spectra of COC molecules in solution are usually unstructured bands with a width of a few tens of nanometers [6].

A COC molecule in ground state absorbs photon with a probability equal to σF, where σ is the absorption cross section (cm^2), and F is the excitation photon flux density ($cm^{-2}\ s^{-1}$). A number of processes lead to relaxation of the excited state.

The typical excited state lifetime of COC molecule is $\tau_F \approx 10^{-9}$ s. Relaxation between vibrational energy levels m and n ($m>n$) within the same electronic level i $S_i^m \rightarrow S_i^n$ is called internal conversion (typical time $\tau_{IC} \approx 10^{-12} \div 10^{-13}$ s). Radiative $S_1 \rightarrow S_0$ transition is called fluorescence. Non-radiative $S_1 \rightarrow S_0$ transitions can also occur; rates of these processes determine fluorescence quantum yield. Nonradiative $S_i \rightarrow T_i$ transitions are called singlet-triplet conversion ($\tau_{ST} \approx 10^{-7}$ s), and radiative

$T_1 \rightarrow S_0$ transitions are called phosphorescence ($\tau_P \approx 10^{-3} \div 10^2$ s). Transitions between energy levels with different multiplicity are spin-forbidden and become partially allowed for COC as the result of spin-orbit coupling.

Radiative transitions from higher energy levels S_i and T_i can also occur, however, for COC, probability of such processes is quite low [6]. When the concentration of fluorescing COC molecules in solution or in an organic complex is high, bimolecular energy transfer processes are possible. One of these processes is singlet-singlet annihilation: when two excited molecules are close enough, energy transfer can occur if the necessary conditions are fulfilled (e.g., in case of fluorescence resonance energy transfer (FRET), the donor's emission band and the acceptor's absorption band must overlap). As the result, one of the molecules comes to the ground state. This effect plays a major role in fluorescent response to pulsed laser excitation of photosynthetic organisms due to high (up to 1 M) local concentration of chlorophyll *a* [12, 17, 18].

Since internal conversion leads to fast deactivation of higher COC molecule energy states S_i and T_i ($i > 1$) and of higher vibrational levels of S_1 and T_1, one can use a three-level model of COC energy states, involving transitions (absorption and excited state relaxation) between S_0, S_1, and T_1 levels (Fig. 30.2).

The balance of S_0, S_1, and T_1 states populations (n_1, n_3, n_2, respectively) for a COC molecule can be described by the system of differential equations (30.1):

$$\begin{cases} \dfrac{\partial n_1(t,\vec{r})}{\partial t} = (K_{31} + K'_{31})n_3(t,\vec{r}) - F(t,\vec{r})\sigma n_1(t,\vec{r}) + \gamma n_3^2(t,\vec{r}) \\ \dfrac{\partial n_2(t,\vec{r})}{\partial t} = K_{32}n_3(t,\vec{r}) \\ \dfrac{\partial n_3(t,\vec{r})}{\partial t} = F(t,\vec{r})\sigma n_1(t,\vec{r}) - (K_{31} + K'_{31} + K_{32})n_3(t,\vec{r}) - \gamma n_3^2(t,\vec{r}) \end{cases} \tag{30.1}$$

where

K_{31}, K'_{31}, K_{32} are the rates of radiative and nonradiative $S_1 \rightarrow S_0$ transitions and the rate of singlet-triplet conversion (see Fig. 30.2)

$\tau^{-1} = K_{31} + K'_{31} + K_{32}$ is the total rate of S_1 state deactivation

σ is the COC molecule's absorption cross section (in the general case, the COC molecule's excitation cross section taking into account all the possible pathways of excitation: direct absorption, energy transfer, etc.)

γ is the constant of the singlet-singlet annihilation rate, caused by energy transfer between two excited fluorophores (Fig. 30.2)

$F(t,\vec{r})$ is the excitation photon flux density

$\vec{r} = \{x, y\}$ are coordinates in the beam cross section

The relation between n_1, n_2, and n_3 is determined by the conservation law:

$$n_0 = n_1 + n_2 + n_3,$$

where n_0 is the total concentration of COC molecules (in cm^{-3}).

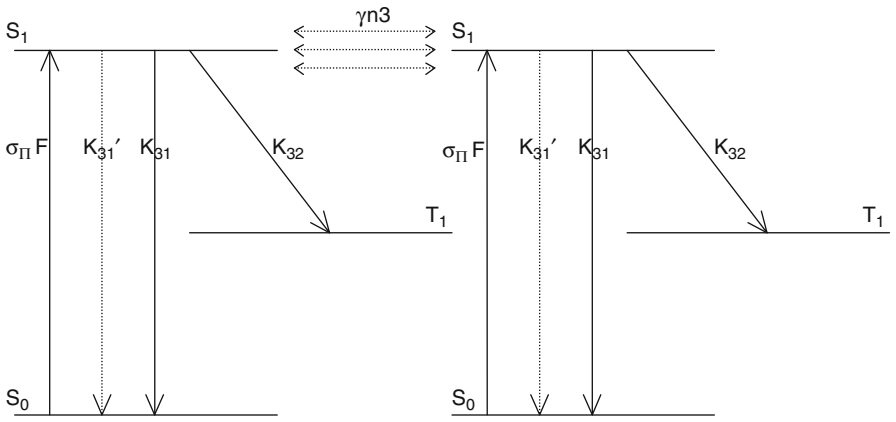

Fig. 30.2 Three-level model of COC molecule energy levels (including singlet-singlet annihilation)

When writing (30.1), the following factors are neglected:

- Excited state absorption from S_1 and T_1 states – if this process does not cause photobleaching (e.g., photoionization), it does not affect the kinetics of the energy level's population due to fast internal conversion,
- Stimulated transitions from S_1 to S_0 (here we suppose the excitation to be non-resonant);
- T_1 ➔ S_0 transitions (it is supposed that the duration of exciting laser pulse $t_{\text{pulse}} << 1/K_{21} << f^{-1}$, where K_{21} is the rate of T_1 state relaxation, and f is the pulse repetition rate; i.e., triplet state T_1 is some kind of "trap," accumulating COC molecules, that completely depopulates between two excitation pulses). Here we consider pulsed laser radiation because of its high photon flux density that can cause nonlinear dependency of fluorescence intensity on the excitation intensity.

Let us consider a diluted solution of the COC molecules that is irradiated with light pulses propagating along the z axis. We regard an optically thin layer of thickness l ($n_0 \cdot \sigma \cdot l << 1$) bounded by two planes perpendicular to the z axis with the coordinates z and $z + l$. Let's consider the fluorescent response of the selected layer to the excitation laser pulse.

The exciting pulse can be represented as a group of photons propagating along the z axis. We suppose the distribution of photons in the beam cross section to be axisymmetric; this allows use of cylindrical coordinates $\{z,\ r\}$ $\left(z = z,\ r^2 = \sqrt{x^2 + y^2}\right)$.

We introduce the distribution function of photons per pulse $g(t/t_p, r/r_0)$, which describes the probability density for a photon of the exciting radiation to be at time t at the point with coordinate r (here, t_p, r_0 are effective pulse duration and beam radius). Let's introduce the following notation: $\xi = t/t_p$, $\rho = r/r_0$, then, by definition,

the probability of a photon to be in the ring of $dV = 2\pi\rho{\cdot}d\rho{\cdot}d\xi$ volume is determined by $g(\xi,\rho)dV$. Therefore, the function $g(\xi,\rho)$ must obey the normalization condition:

$$\int_{-\infty}^{+\infty}\int_{-\infty}^{+\infty} g(\xi,\ \rho)\cdot 2\pi\rho\cdot d\rho\cdot d\xi = 1. \tag{30.2}$$

Let $g(\xi, \rho)$ be a factorized distribution $g(\xi, \rho) = g_\xi(\xi){\cdot}g_\rho(\rho)$. The effective pulse duration τ_p and the beam radius r_0 can be defined as follows:

$$\begin{aligned} g_\xi(\pm 0.5) &= 0.5\cdot g_\xi(0)\\ g_\rho(1) &= 0.5\cdot g_\rho(0) \end{aligned} \tag{30.3}$$

Possible $g_\xi(\xi)$ distributions include Gauss distribution in time

$$g_{\xi\Gamma}(\xi) = \sqrt{\frac{4\cdot\ln(2)}{\pi}}\cdot\exp(-4\cdot\ln(2)\cdot\xi^2) \tag{30.4}$$

and in the beam cross section

$$g_{\rho\Gamma}(\rho) = \frac{\ln(2)}{\pi}\cdot\exp(-\ln(2)\cdot\rho^2). \tag{30.5}$$

These distribution functions [(30.4) and (30.5)] satisfy (30.3), and their combinations satisfy (30.2).

Let us select a ring volume $dV = 2\pi\rho{\cdot}d\rho{\cdot}d\xi$. The number of exciting pulse photons in dV is $N_{\mathrm{dV}} = F(t, r){\cdot}2\pi r{\cdot}dr{\cdot}dt$, where $F(t, r)$ is the photon flux density. From the other side, $N_{\mathrm{dV}} = N{\cdot}\mathrm{g}(\xi,\rho){\cdot}2\pi\rho{\cdot}d\rho{\cdot}d\xi$, where N stands for the total number of photons in the pulse. Hence, $F(t,r)\cdot r_0^2\cdot t_p = N\cdot g(\xi,\rho)$. The value $F_{eff} = \frac{N}{t_p\pi r_0^2}$ is called the effective photon flux density of the exciting radiation and

$$F(t,r) = \pi\cdot g(t/t_p, r/r_0)\cdot F_{eff} = \pi\cdot g(\xi,\rho)\cdot F_{eff}. \tag{30.6}$$

In cylindrical coordinates $\left(z = z,\ r^2 = \sqrt{x^2+y^2}\right)$, assuming an optically thin layer system, (30.1) is transformed into

$$\begin{cases} \dfrac{\partial n_1(t,r)}{\partial t} = (K_{31}+K'_{31})n_3(t,r) - \pi\cdot g(t/t_p, r/r_0)\cdot F_{eff}\sigma n_1(t,r) + \gamma n_3^2(t,r)\\ \dfrac{\partial n_2(t,r)}{\partial t} = K_{32}n_3(t,r)\\ \dfrac{\partial n_3(t,r)}{\partial t} = \pi\cdot g(t/t_p, r/r_0)\cdot F_{eff}\sigma n_1(t,r) - (K_{31}+K'_{31}+K_{32})n_3(t,r) - \gamma n_3^2(t,r) \end{cases} \tag{30.7}$$

Integrating the system (30.7) and taking into account the conservation law, one can obtain an expression for the population of the first excited singlet state of fluorescent molecules $n_3(t, \boldsymbol{r})$. Using this expression, it is possible to find the number of fluorescence photons emitted from the selected layer of the solution as a result of excitation by the laser pulse:

$$\begin{aligned} N_{fl} &= K_{31} \times \int_{z}^{z+l} dz \cdot \int_{0}^{\infty} 2\pi r \cdot dr \cdot \int_{-\infty}^{\infty} n_3\left(K_{31}, K'_{31}, K_{32}, \sigma, \gamma, F_{eff}, t, r\right) \cdot dt \\ &= K_{31} \cdot l \times \int_{0}^{\infty} 2\pi r \cdot dr \cdot \int_{-\infty}^{\infty} n_3\left(K_{31}, K'_{31}, K_{32}, \sigma, \gamma, F_{eff}, t, r\right) \cdot dt \end{aligned} \tag{30.8}$$

30.2.2 Fluorescence Saturation of COC Under Pulsed Laser Excitation. Basics of the Nonlinear Fluorometry

With increasing intensity of the exciting radiation, the dependence of COC molecules' fluorescence photons [see (30.8)] on the photon flux density becomes nonlinear (Fig. 30.3a). This effect is called fluorescence saturation. In the framework of the adopted three-level model (for single-component solution of COC), there are two basic mechanisms of fluorescence saturation [9, 12, 17]: depletion of the ground state of fluorescent molecules (absorption bleaching) and singlet-singlet annihilation.

Nonlinear laser fluorometry is based on the fluorescence saturation effect and operates with the measured dependence of the number of fluorescence photons N_{fl} on the photon flux density F of the exciting laser radiation – N_{fl}(F). At typical F values for pulsed lasers ($F \geq 10^{20}$ cm^{-2} s^{-1}), deviation of $N_{fl}(F)$ from the linear law appears, in varying degrees for different COC. For diluted solutions of organic dyes, nonlinearity becomes significant at F values $F \geq 10^{24}$cm^{-2}c^{-1} [9] and for objects with a high local concentration of fluorophores (e.g., photosynthetic organisms), it is already apparent at $F \geq 10^{19}$ cm^{-2} s^{-1} [12, 17].

The next step is the inverse problem solution: determination of photophysical parameters used in the model describing experimental fluorescence saturation curves $N_{fl}(F)$. As usual, the inverse problem solution consists of two stages: direct problem solution (evaluation of $N_{fl}(F)$ for a given set of photophysical parameters) and the inverse problem solution itself: determination of the set of parameters that gives minimum discrepancy between theoretical and experimental saturation curves. For this purpose, different algorithms – the traditional variational, such as gradient descent methods and nonlinear regression, and neural networks [10] – are used. Some unique capabilities of nonlinear fluorometry (NLF) will be presented in Sect. 30.3 using the example of concrete proteins. As with any other method, NLF has its limitations: because of the monotonous character of the saturation curves,

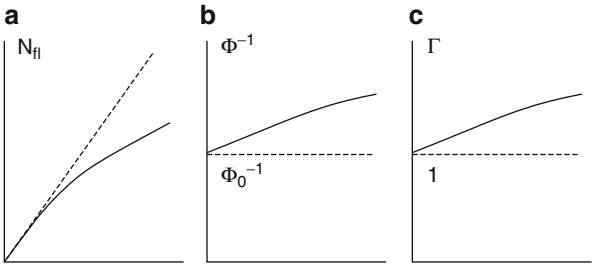

Fig. 30.3 Fluorescence saturation curve in different axes: (**a**) $N_{fl}(F)$, (**b**) $\Phi^{-1}(F)$, (**c**) $\Gamma(F)$. Dependencies in the absence of fluorescence saturation are shown with *dotted lines*

the dimension of an inverse problem with a sustainable solution is no more than three (detailed analysis of sustainability and uniqueness of NLF inverse problem solution is given in [11]). This limitation is partially overcome in the so-called matrix method of laser fluorometry, synthesizing nonlinear and time-resolved (kinetic) fluorometry [19]. Fundamentals of this method are described in Sect. 30.2.4, which is preceded by a description of the method of time-resolved fluorometry (Sect. 30.2.3).

In real experiments, the value $N_{fl}(F)$ is measured in arbitrary units (a.u.), since the procedure for measuring the absolute values of fluorescence photons is cumbersome and fraught with errors. In order to obtain quantities that can be measured in absolute terms and compared with those calculated from the adopted model, it is necessary to make the normalization of the number of detected fluorescence protons N_{fl} some reference signal N_{ref} that depends linearly on the photon flux density of exciting radiation. The intensity of laser radiation measured by the second photodetector or the signal of Raman scattering (RS) of light by water molecules or other solvent [9, 20] can be used as a reference signal. The ratio $\Phi = N_{fl}/N_{\text{ref}}$ is called the fluorescence parameter.

To characterize the degree of fluorescence saturation, the saturation factor $\Gamma = \frac{N_{fl}^0}{N_{fl}}$ is introduced, where $N_{fl}^0 = F \times \lim\limits_{F \to 0} \frac{dN_{fl}}{dF}$ is the number of photons that would have been emitted by the molecule in the absence of saturation. Fluorescent parameter Φ is connected with Γ by the following equation: $\Gamma = \frac{\Phi_0}{\Phi}$, where $\Phi_0 = \lim\limits_{F \to 0} \Phi(F)$ is the unsaturated fluorescence parameter that does not depend on F. In absence of fluorescence saturation, $N_{fl} \sim F$ and $\Gamma = 1$. When $N_{fl}(F)$ becomes nonlinear, $\Gamma(F)$ ceases to be a unit (Fig. 30.3). The dependencies $N_{fl}(F)$ (Fig. 30.3a), $\Phi^{-1}(F)$ (Fig. 30.3b), and $\Gamma(F)$ (Fig. 30.3c) are called fluorescence saturation curves in corresponding axes.

30.2.3 Fluorescence Kinetics of COC Molecules. Principles of Time-Resolved Fluorometry

The classical method of time-resolved fluorometry [2] is based on analysis of the fluorescence decay curves after the exciting pulse with much shorter

duration than the lifetime of the excited state. For typical COC molecules, this method requires the use of picosecond pulses. However, information about the relaxation of the excited state of COC molecules can be also obtained with nanosecond excitation.

In Ref. [21], the suggested variant of time-resolved fluorometry COC solution is excited laser pulses with duration $\tau_p = 10$ ns. The fluorescence signal is detected with intensified CCD camera with mini/mum gate width $\tau_{gate} = 10$ ns and gating resolution $\Delta\tau = 2.5$ ns. It was shown that, using this equipment it, becomes possible to determine COC molecules' lifetimes down to 1 ns, despite the fact of large τ_p and τ_{gate} values.

Here, the dependence of the number of photons in the ICCD gate t_g on the delay time t_{del} after the exciting laser pulse is called the kinetic curve. According to (30.8), $N_{fl}(t_{del})$ is given by:

$$N_{fl} = K_{31} \cdot l \times \int_0^{\infty} 2\pi r \cdot dr \int_{-t_g/2+\tau_{del}}^{t_g/2+\tau_{del}} n_3(t,r) \cdot dt \tag{30.9}$$

Delay time t_{del} changes discretely proportional to the number of the gating steps i: $t_{del} = i \times t_{\text{step}}$.

When using this technique, the key point is selection of the zero point, that is, the moment when $t_{del} = 0$; for example, this point can be chosen from the condition that at $t_{del} = 0$ the maximum of the laser pulse and the center of the ICCD gate coincide. This point can be chosen using the maximum of Raman scattering by water molecules as a reference (RS signal is almost inertialess; the elementary act of scattering occurs at $10^{-11} - 10^{-12}$ s timescales).

Fluorescence intensity is measured in a.u., so in order to compare for experimental and calculated kinetic curves the normalized values of intensity are used:

$$I_{fl}(t_{del}) = \frac{N_{fl}(t_{del})}{N_{fl}(0)}$$

where $Nfl(t_{del})$ is the number of photons registered at t_{del} delay at the same gate width. This normalization is used during processing of experimental data.

30.2.4 Matrix Method in COC Fluorometry

As already mentioned, capabilities of NLF are limited by the number of photophysical parameters that can be recovered from smooth fluorescence saturation curves. In many cases, this can be enough, for example, in the case of monofluorophoric solution absorption cross section (in absence of a priori information about concentration; see Sect. 30.3 for details), excited state lifetime, the

rate of singlet-triplet conversion, or the rate of singlet-singlet annihilation can be determined. However, in case of a bifluorophoric system when energy transfer appears, this set of parameters can appear to be insufficient. This situation is mathematically described by a system of kinetic equations:

$$\begin{cases} \dfrac{dn_1}{dt} = F(t)\sigma_1(n_{01} - n_1) - \dfrac{n_1}{\tau} - \gamma n_1^2 - K_{12}(n_{02} - n_2) \\ \dfrac{dn_2}{dt} = F(t)\sigma_2(n_{02} - n_2) - \dfrac{n_2}{\tau} - \gamma n_2^2 + K_{12}(n_{02} - n_2) \end{cases} \tag{30.10}$$

with the following abbreviations:
n_1, n_2 – concentrations of the excited molecules of the corresponding fluorophores;
n_{01}, n_{02} – initial concentrations of the molecules of the corresponding fluorophores;
τ_1, τ_2 – lifetimes of the excited molecules of the corresponding fluorophores;
γ_1, γ_2 – constants of singlet-singlet annihilation of the corresponding fluorophores;
σ_1, σ_2 – excitation cross sections of the corresponding fluorophores;
$F(t)$ – photon flux density of the exciting radiation;
K_{12} – constant of intermolecular energy transfer from the first to the second fluorophore.

Having determined $n_1(t,F)$ and $n_2(t,F)$, it is possible to calculate the fluorescence intensity $I(F,T)$ in a receiver gate delayed for time T with respect to the exciting laser pulse for the given value of photon flux density F [21].

In this model we do not separate singlet-triplet conversion from the common channel of intermolecular relaxation of excited state of fluorophores, that is, from the total time of this relaxation, τ_1 and τ_2. Nevertheless, there are nine model parameters, which cannot be determined simultaneously neither with the kinetic fluorometry method, nor with the nonlinear fluorometry method, nor by the sequential use of these methods. These considerations have led to the idea to perform a synthesis of these methods [19]. To do so, the following matrix needs to be measured:

$$M_{FT} = \begin{bmatrix} I_{F_1T_1} & \dots & I_{F_1T_t} \\ \vdots & \vdots & \vdots \\ I_{F_WT_1} & \dots & I_{F_WT_t} \end{bmatrix}$$

where I_{FnTm} is the fluorescence intensity of the COC mixture for the exciting radiation photon flow density F_n and for the gate delayed for time T_m with respect to the laser pulse.

The rows of this matrix are the points on kinetic curves at different photon flux densities F; the columns are the points on fluorescence saturation curves at different gate delays T. The range of F should be selected in such a way that, at its minimal value, there would be no saturation of fluorescence, and at its maximum value saturation would be significant. The degree of saturation at maximum F is chosen based on the peculiarities of the specific problem.

From physical considerations, it may be expected that different matrix elements have different dependences on photo-physical parameters. Consequently, under rational choice of matrix elements, all photo-physical parameters can be determined.

It should be noted that this approach is in principle different from the matrix method, suggested in [22, 23] and aimed at determination of partial concentrations of components in a mixture where the following matrix is used:

$$M_{\lambda T} = \begin{bmatrix} I_{\lambda_1 T_1} & \dots & I_{\lambda_1 T_t} \\ \vdots & \vdots & \vdots \\ I_{\lambda_W T_1} & \dots & I_{\lambda_W T_t} \end{bmatrix}$$

Here, the matrix elements are the values of intensity measured at different wavelength within the overall fluorescence band at different ICCD gate delay with respect to the laser pulse.

30.2.5 Laser Fluorometry of Localized Donor-Acceptor Pairs. Collective States of Donor-Acceptor Pair

The systems with excitation energy transfer in which the donor has only one possible acceptor (localized donor-acceptor pairs) are finding increasing wider application [24, 25]. Commonly, the systems of this kind are constructed artificially out of pairs of organic compounds (e.g., out of dye molecules or fluorescent protein macromolecules). A description of the fluorescence response of such systems in terms of the conventional approach becomes inapplicable, because the situation is possible when the donor and the acceptor of a LDA pair are simultaneously in an excited state; therefore, the energy transfer in the framework of a conventional scheme [see (30.10)] is impossible. The model presented in this section makes it possible to describe the energy transfer inside a LDA pair, but disregarding the energy transfer between the pairs.

We employ the following notations: S_{0D}, S_{1D} are the ground and the first excited states of the donor, S_{0A}, S_{1A} are the same for the acceptor. Let us to introduce a notion of the collective states of a LDA pair, each of these states simultaneously describes both the donor state and the acceptor state:

- Collective state 1: the donor and the acceptor are in the ground state S_{0D} and S_{0A}, respectively; the concentration of such molecules is denoted as $n_1 \equiv n_1(t, \vec{r})$;
- Collective state 2: the donor is in the state S_{1D}, and the acceptor is in the state S_{0A}; the concentration of such molecules is denoted as $n_2 \equiv n_2(t, \vec{r})$;
- Collective state 3: the donor is in the state S_{0D}, and the acceptor is in the state S_{1A}; the concentration of such molecules is denoted as $n_3 \equiv n_3(t, \vec{r})$;
- Collective state 4: the donor and the acceptor are in the first excited state S_{1D} and S_{1A}, respectively; the concentration of such molecules is denoted as $n_4 \equiv n_4(t, \vec{r})$

The collective states of a LDA pair can be illustrated by the diagrams, see Fig. 30.4.

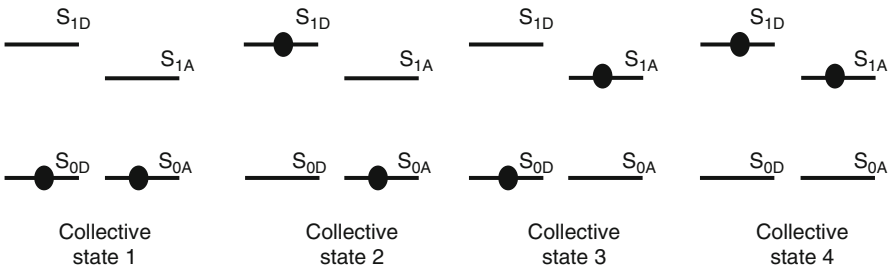

Fig. 30.4 The collective states of the localized donor-acceptor pair (in each collective state the left scheme of the energy levels is attributed to the donor of the LDA pair (levels S_{0D} and S_{1D}) and the right one to the acceptor (levels S_{0A} and S_{1A}))

The dynamics of variation in the concentrations of these four collective states of the LDA pair (disregarding singlet-triplet conversion and single-singlet annihilation process) is mathematically described by the following system of the kinetic (30.11):

$$\begin{cases} \dfrac{\partial n_1}{\partial t} = -F(t,\vec{r}) \cdot (\sigma_D + \sigma_A) \cdot n_1 + \dfrac{n_2}{\tau_3^D} + \dfrac{n_3}{\tau_3^A} \\ \dfrac{\partial n_2}{\partial t} = -F(t,\vec{r}) \cdot \sigma_A \cdot n_2 - \dfrac{n_2}{\tau_3^D} - K_{DA} \cdot n_2 + F(t,\vec{r}) \cdot \sigma_D \cdot n_1 + \dfrac{n_4}{\tau_3^A} \\ \dfrac{\partial n_3}{\partial t} = -F(t,\vec{r}) \cdot \sigma_D \cdot n_3 - \dfrac{n_3}{\tau_3^A} + F(t,\vec{r}) \cdot \sigma_A \cdot n_1 + \dfrac{n_4}{\tau_3^D} + K_{DA} \cdot n_2 \\ \dfrac{\partial n_4}{\partial t} = F(t,\vec{r}) \cdot \sigma_A \cdot n_2 + F(t,\vec{r}) \cdot \sigma_D \cdot n_3 - \dfrac{n_4}{\tau_3^D} - \dfrac{n_4}{\tau_3^A} \\ n_1 + n_2 + n_3 + n_4 = n_0, \end{cases} \tag{30.11}$$

where the symbols D and A denote the donor and the acceptor, respectively; τ is the lifetime of excitation state of the donor or acceptor molecules; σ is the absorption cross section corresponding to the $S_0 \rightarrow S_1$ transition; K_{DA} is the rate of the energy transfer from the excited donor to the unexcited acceptor; n_0 is the total concentration of molecules containing a LDA pair.

It should be noted that that the parameter K_{DA} in (30.11) has the meaning of the energy transfer rate, whereas in the conventional model (30.10) it is the constant of the energy transfer rate, that is, the rate normalized to a unitary concentration of the unexcited acceptor molecules. This is the consequence of the fact that the model described by (30.11) suggests the presence of only one donor and one acceptor in a macromolecule (it should be noted that the model can be generalized for the case when a macromolecule contains several donors and acceptors). In this case, the energy transfer rate can assume two fixed values: $K_{DA} = 0$ (in the collective state 4) and $K_{DA} = \text{const}$ (in the collective state 2). In the conventional model, the donor is surrounded by a large quantity of the acceptor molecules and,

consequently, the rate of energy transfer can assume a continuous series of values from 0 to some maximum value, which is equal to $K_{DA}{}^{*} \times M_{0A}$, here $K_{DA}{}^{*}$ is the constant of energy transfer rate, and M_{0A} is the concentration of the acceptor molecules.

Knowing the law of variation in the concentration of fluorescent molecules in the excited state, one can calculate the number of fluorescence photons N_{Fl}, emitted under the influence of a laser pulse:

For the donor:

$$N_{Fl}^{D}(\lambda) \propto \int_{0}^{\infty} 2\pi r \cdot dr \int_{-\infty}^{+\infty} (n_2(t,r) + n_4(t,r))dt; \tag{30.12}$$

For the acceptor:

$$N_{Fl}^{A}(\lambda) \propto \int_{0}^{\infty} 2\pi r \cdot dr \int_{-\infty}^{+\infty} (n_3(t,r) + n_4(t,r))dt. \tag{30.13}$$

In the model described by (30.11), the fluorescence saturation occurs due to the finite time of return of fluorescent molecules from the excited state S_1 to the ground state S_0, and due to a decrease in the number of molecules in the collective state 2 (the saturation of the energy transfer channel). As the conventional model, model (30.11), operating with the collective states of a LDA pair, could be supplemented with other mechanisms of the fluorescence saturation (the singlet-triplet conversion, singlet-singlet annihilation, photochemical processes in an excited state, etc.).

30.3 Laser Fluorescent Spectroscopy of Proteins

30.3.1 Optical Properties of Protein Macromolecules

It is well known [26] that protein molecules obtain intrinsic luminescence in the UV region of spectrum due to the presence of aromatic amino acids – tryptophan (Trp), tyrosine (Tyr), and phenylalanine (Phe). About 90 % of the total fluorescence of proteins is usually due to tryptophan residues. This natural fluorophore is extremely sensitive to the polarity of the environment. Spectral shifts of its absorption and fluorescence bands are often the consequence of several phenomena, among which are the ligand binding, protein-protein association and denaturation. Proteins absorb light near 280 nm, the maxima of fluorescence spectra lie in the region 320–350 nm (Fig. 30.5). Excited state lifetimes of tryptophan residues usually ranged from 1 to 6 ns.

Tyrosine fluoresces intensively in solution, but its emission intensity in proteins is much weaker. Protein denaturation usually increases tyrosine emission.

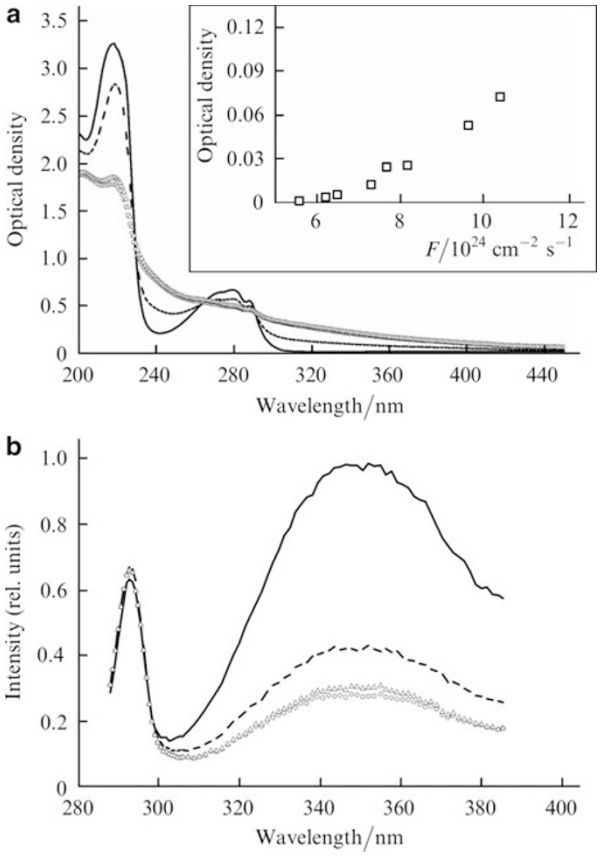

Fig. 30.5 Irreversible changes in the absorption (**a**) and fluorescence (**b**) spectra of the tryptophan solution during its irradiation by UV light: before irradiation (*solid curve*), after irradiation for 15 min (*dashed curve*), after irradiation for 30 min (*circles*), and within 6 h after the end of 30-min irradiation (*triangles*) for the photon flux density $F = 10^{25}$ cm^{2}s^{-1}. The inset shows the dependence of the change in the optical density of the aqueous solution of tryptophan at 278 nm due to the photoproduct formation on the exciting photon flux density. The irradiation time is 30 min [27]

Phenylalanine's fluorescence quantum yield in proteins is small (less than 1 %), so its impact on protein fluorescence can usually be neglected.

A detailed analysis of the intrinsic fluorescence of proteins is hampered by the number of factors that affect the fluorescence and the presence of several different aromatic amino acid residues in one protein molecule. Since each residue is in a different environment, its spectral properties may differ. Emission spectra of all residues overlap, and it is difficult to separate the spectral contributions of each of them, for example, in a multitryptophan protein. In addition, the emission spectra and fluorescence relaxation kinetics are rather complicated, even for free tryptophan and proteins containing a single tryptophan residue. For example, for most proteins with a single tryptophan residue multiexponential fluorescence decay is observed; for this reason we can't simply interpret the data of time-resolved fluorometry in terms of the behavior of individual residues in multitryptophan proteins. A detailed review of data on amino acids and proteins fluorescence can be found, for example, in Ref. [26].

30.3.2 Nonlinear Laser Fluorometry of Tryptophan

As already noted, many proteins fluoresce in the near UV region due to the presence of tryptophan, tyrosine, and phenylalanine residues (aromatic amino acid residues) [26]. Because the parameters of fluorescence spectra (position, shape, intensity, etc.) of aromatic amino acids (fluorophores) characterize their interaction with the environment, they can be used to obtain information about the properties of protein molecules. To obtain more complete information, it is also important to know the molecular photophysical parameters of fluorophores such as absorption cross sections, singlet-triplet conversion constants, and so on. Of special importance is studying the nature of fluorescence of tryptophan molecules because this fluorescence dominates in the so-called intrinsic fluorescence of proteins [26].

Although the fluorescence of tryptophan in solutions and proteins has been investigated in many papers (see review in Ref. [26]), the nature of the fluorescence band of this amino acid cannot be considered explained so far. The determination of the entire set of photophysical parameters of a tryptophan molecule and their dependence on the environment factors is promising for the development of the method of fluorescence diagnostics of proteins.

In Ref. [27] the results of measuring the molecular photophysical parameters of tryptophan in aqueous solution by the method of nanosecond laser fluorometry based on the simultaneous recording (by using one laser spectrometer) of the kinetic and fluorescence saturation curves are presented. The solution of L-tryptophan (Ajinomoto, Japan) in mQ water (MilliPor, USA) was studied. Absorption spectra were recorded at the tryptophan concentration of 1.3×10^{-4} M; fluorescence spectra and fluorescence saturation curves were obtained at the tryptophan concentration of 2×10^{-9} M. All the experiments were carried out at temperature 25 °C ± 1 °C.

Excitation of tryptophan molecules by UV radiation can induce a number of photophysical processes and photochemical reactions involving the excited state. Although the photophysical parameters of tryptophan molecules have been studied in many papers, the mechanisms of their phototransformations have not been completely established. The values of photophysical parameters corresponding to these processes reported in the literature differ considerably [28–33] (see Table 30.1 below).

The following deactivation mechanisms of the first excited singlet state can be distinguished, which affect the fluorescence response of a low-concentration tryptophan solution excited by nanosecond laser pulses:

1. Radiative and nonradiative transitions to the ground state
2. Singlet-triplet conversion
3. Spontaneous ionization
4. Photoionization. This process was not considered in detail anywhere; it was also pointed out that it occurs and ionization products are similar to products formed upon one-step ionization [28–30]. This process, as with process 3, is reversible, with recombination times at the micro-to-millisecond scale [29].

Table 30.1 Photophysical parameters of tryptophan molecules in an aqueous solution.

Parameter	Values	
	NLF-based method [27]	Other (linear) methods
τ_3, ns	2.8 ± 1	3.13 (amplitude = 0.93), 0.53 [28]
σ, 10^{-17} cm^2	1.6 ± 0.3	1.9 [28]
$\eta_T + \eta_i$	0.17 ± 0.5	$\eta_T = 0.12$ [28]; $\eta_i = 0.25$ [29]; $\eta_i = 0.08$ [28, 30]
$K_{32} + K_{3i}$, 10^7 c^{-1}	6 ± 2	
$(\sigma_{3i} + \sigma_{ph})$, 10^{-18} cm^2	2.2 ± 0.7	

5. Formation of a non-recoverable photoproduct. The existence of such an irreversible mechanism is pointed out in [28]; however, like process 4, it has not been quantitatively studied. It seems that this process, as process 4, is caused by the absorption of a photon by a tryptophan molecule in the first excited singlet state (and, hence, is a two-step process as a whole). This is confirmed by the fact that the dependence of the product formation rate on the radiation intensity deviates from a linear dependence (inset in Fig. 30.5a), and the product formation is manifested in a gradual decrease in the fluorescence intensity (during UV irradiation) and optical density in the first and second singlet absorption bands of a sample (Fig. 30.5).

The two-step processes 4 and 5 are poorly studied since the experimental measurement of the quantum yield of ions and a photoproduct in the case of a two-photon reaction involves considerable difficulties because it is necessary to know the concentration of excited molecules absorbing the second photon and also their extinction coefficient at the excitation wavelength. Thus, it is difficult to describe these processes quantitatively within the framework of traditional classical approaches. The authors of most papers (e.g., on flash photolysis [29, 30]) deliberately selected the energy parameters of setups to minimize the contributions of two-step processes (specially specifying this fact) to the quantitative characteristics being determined. When molecular photophysical parameters are measured by the method of nonlinear fluorometry upon excitation by high-power radiation, processes 4 and 5 can make a noticeable contribution to the fluorescence response, and therefore their neglect can lead to errors in the measurements of other parameters. Moreover, the consideration of these processes in the method of nonlinear fluorometry allows one to obtain their quantitative parameters.

In the laser fluorometer used in Refs. [13–15, 27], fluorescence was excited by 10-ns, 0.7-mJ, 266-nm fourth-harmonic pulses from a Nd:YAG laser with a pulse repetition rate of 10 Hz. Fluorescence was recorded with an optical multichannel analyzer consisting of a polychromator and a multichannel camera (DeltaTech, Moscow State University Scientific Park), which gave a two-dimensional optical image in the plane of the polychromator exit slit. The camera was coupled with a PC equipped with the software allowing operation both in the continuous (nonlinear fluorometry) and gated (kinetic fluorometry) regimes. The gate duration was 10 ns, the delay time step was 2.5 ns. The fluorescence intensity was measured

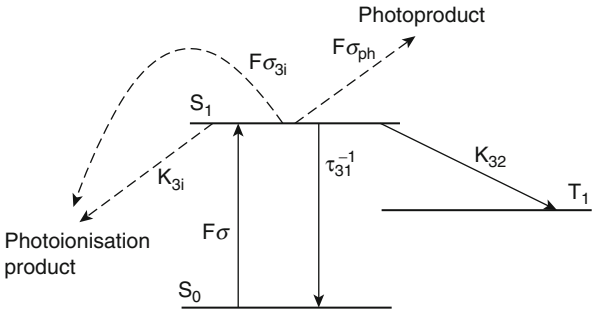

Fig. 30.6 Energy level diagram of a polyatomic organic molecule, corresponding to the system of kinetic (balance) (30.13). The arrows indicate processes considered above ($F\sigma$ is the probability of photon absorption from the S_0 state; ${\tau_{31}}^{-1}$ is the total rate of radiative and nonradiative transitions from the excited S_1 single t state to the S_0 ground state; K_{32} and K_{3i} are the rate constants of singlet-singlet conversion and spontaneous ionization, respectively; $F\sigma_{3i}$ and $F\sigma_{ph}$ are the probabilities of induced photoionization and product formation, respectively)

by varying the laser photon flux density F from 2×10^{24} to 5×10^{25} cm^2s^{-1}. For a fixed value of F (and a fixed delay time in the case of kinetic measurements [21]), the fluorescence signal was obtained by averaging over 100 pulses. The dynamics of photoproduct formation was studied by the methods of absorption and fluorescence spectroscopy by using a tryptophan solution of volume 3 mL. Nonlinear and kinetic fluorometry was performed by using a continuous-flow system to exclude the photoproduct accumulation. Absorption spectra were recorded with a Lambda 25 PerkinElmer spectrophotometer.

The model of a fluorescence response, which is used in the methods of nonlinear and kinetic fluorometry and takes into account processes pointed out above, is described by the system of kinetic equations for populations of the energy states of a polyatomic organic molecule (Fig. 30.6), where, in comparison with models from Sect. 30.4, photophysical processes involving the excited state are taken into account:

$$\begin{cases} \dfrac{\partial n_3(t,\vec{r})}{\partial t} = F(t,\vec{r})\sigma \cdot n_1(t,\vec{r}) - \dfrac{n_3(t,\vec{r})}{\tau_{31}} - (K_{32} + K_{3i})n_3(t,\vec{r}) - \\ - F(t,\vec{r})(\sigma_{3i} + \sigma_{ph})n_3(t,\vec{r}) \\ \dfrac{\partial n_2(t,\vec{r})}{\partial t} = K_{32}n_3(t,\vec{r}) \\ \dfrac{\partial n_i(t,\vec{r})}{\partial t} = K_{3i}n_3(t,\vec{r}) + F(t,\vec{r})\sigma_{3i}n_3(t,\vec{r}) \\ \dfrac{\partial n_{ph}(t,\vec{r})}{\partial t} = F(t,\vec{r})\sigma_{ph}n_3(t,\vec{r}) \\ n_0 = n_1 + n_2 + n_3 + n_i + n_{ph} \end{cases} \tag{30.14}$$

where n_0 is the sum of concentrations of initial polyatomic molecules and their photoproducts; n_3, n_2, and n_1 are concentrations of molecules in the first excited S_1

singlet (level 3), the first excited T_1 triplet (level 2), and the S_0 ground (level 1) states, respectively; n_i is the total concentration of reversibly ionized and photoionized molecules; n_{ph} is the concentration of reversibly photoionized and irreversibly photodegraded molecules; $F(t, \boldsymbol{r})$ is the photon flux density of exciting radiation at the instant t at the point with coordinate $\boldsymbol{r} = \{x, y\}$ in the plane perpendicular to the laser beam direction (the dependence of parameters on the coordinate z along the beam direction is neglected, i.e., the optically thin layer approximation is used); σ is the absorption cross section of the fluorophore; $\tau_{31} = 1/(K_{31} + K'_{31})$, where K_{31} and K'_{31} are the rate constants of radiative and nonradiative transitions from the excited S_1 singlet state to the S_0 ground state (level 1); K_{32} is the rate constant of singlet-triplet conversion; K_{3i} is the rate constant of spontaneous ionization from the S_1 state; σ_{3i} and σ_{ph} are the cross sections for photoionization and photodegradation of molecules from the S_1 state induced by irradiation.

The total lifetime of a molecule in the S_1 state (fluorescence decay time) in this model is described by the expression

$$\tau_3{}^{-1} \equiv K_3 = \tau_{31}{}^{-1} + K_{32} + K_{3i} + F \cdot (\sigma_{3i} + \sigma_{ph}), \tag{30.15}$$

which at low excitation intensities (when the absorption of radiation by molecules in the S_1 state can be neglected) has the form

$$\tau_3{}^{-1} \equiv K_3 = \tau_{31}{}^{-1} + K_{32} + K_{3i}. \tag{30.16}$$

The lifetimes of the $T_1 \rightarrow S_0$ transition and recombination of ions can lie in the micro- and millisecond ranges, which greatly exceeds the laser pulse duration but is smaller than the time between laser pulses (0.1 s). This allows us to neglect these processes in the system, described by (30.15) [28–30].

Knowing variations in molecular concentrations n_3(t, $\boldsymbol{r}$), we can calculate the number N_{fl} of fluorescence photons emitted upon excitation by a laser pulse. For an axially symmetric beam, N_{fl} is determined with (30.8).

The fluorescence saturation in the model under study is caused by a finite $S_1 \rightarrow S_0$ fluorescence decay time, the singlet-triplet conversion, mechanisms of ionization and photoionization and the formation of a photoproduct. The method of nonlinear fluorometry involves the measurement (by solving the inverse problem) of molecular photophysical parameters of organic compounds from the saturation curve $N_{fl}(F)$. It is convenient to normalize the number N_{fl} of detected fluorescence photons to the reference signal N_{ref}, which can be a Raman scattering line of water (or other solvent).

In principle, all photophysical parameters of the model, described by (30.14), can be determined from the fluorescence saturation curve. However, the practical stability of the solution of the corresponding inverse problem allows one, at present, to determine no more than three parameters [10, 11]. Therefore, along with the measurement of the saturation curve, we recorded the fluorescence kinetics by using the same laser spectrometer.

The lifetime τ_3 found from the kinetic curve $N_{fl}(t_{del})$ recorded at low-intensity laser pulses ($F < 10^{23}$ cm^{2}s^{-1}) was a fixed parameter in the model describing the saturation curve. The combined use of kinetic and nonlinear fluorometry allows us to solve the four-parameter inverse problem with a sufficient practical stability. However, as follows from (30.16), by using the method of kinetic fluorometry, two parameters, ${\alpha_3}^{-1} = {\tau_{31}}^{-1} + K_{32} + K_{3i}$ and $\beta \equiv (\sigma_{3i} + \sigma_{ph})$, can also be determined by recording several (minimum, two) kinetic curves for different values of F.

It was shown in papers [31, 32] that the fluorescence decay of the aqueous solution of tryptophan excited by picosecond laser pulses was described by two exponentials: the long-lived (~3 ns) component making a dominant contribution (85–95 %) and the short-lived (~0.5 ns) component. So far, no convincing mechanisms were proposed that would predict the nonexponential fluorescence decay of tryptophan. For this reason, and also taking into account the nanosecond duration of the exciting pulse and the nanosecond time resolution of a detector, in [27] the inverse problem of kinetic fluorometry by using a model with one excited-state lifetime $\tau_3 = ({\tau_{31}}^{-1} + K_{32} + K_{3i})^{-1}$ was solved.

Figure 30.7 presents one of the kinetic curves obtained in [27]. The processing of such curves by the variation method gave $\tau_3 = 2.8 \pm 1$.

Figure 30.8 shows one of the fluorescence saturation curves. The solution of the three-parametric inverse problem with the fixed parameter $\tau_3 = 2.8$ ns gave the following values of the other model parameters: $\sigma = (1.6 \pm 0.3) \times 10^{-17}$ cm^2; $\sigma_{3i} + \sigma_{ph} = (2.2 \pm 0.7) \times 10^{-18}$ cm^2; $K_{32} + K_{3i} = (6 \pm 2) \times 10^7$ s^{-1}. These values give the sum of triplet and ionization quantum yields $(\eta_T + \eta_i) = 0.17 \pm 0.5$.

The parameter $\beta \equiv (\sigma_{3i} + \sigma_{ph})$ was also determined from kinetic measurements by measuring two kinetic curves for low and high values of F. For $F = 10^{23}$ cm^{-2} s^{-1}, the calculated lifetime was 2.8 ± 1 ns, while for $F = 10^{26}$ cm^{-2} s^{-1} this time was $\tau_3 = 2 \pm 1$ ns. Then, by using (30.16), $\sigma_{3i} + \sigma_{ph} = (1.2 \pm 0.4) \times 10^{-18}$ was determined, which agrees (taking the confidence interval into account) with the value obtained from the saturation curve.

Since the influence of the intersystem crossing (the rate K_{32}) and spontaneous ionization (the rate K_{3i}) on the fluorescence kinetics and saturation curves is indistinguishable, one can determine within the framework of the NLF method only the total rate of these processes. A similar situation takes place for cross sections for reversible photoionization (σ_{3i}) and formation of a stable photoproduct (σ_{ph}).

Table 30.1 compares the results obtained [27] with the use of the complex method including NLF with the data, obtained with the use of classical spectroscopy.

30.3.3 Nonlinear Laser Fluorometry of Proteins Containing One and Two Tryptophan Residues. Application of the Formalism of Localized Donor-Acceptor Pairs

Tryptophan is used as a natural "intrinsic tag" whose fluorescence can bring information about the changes in the protein molecule properties under an external action [26].

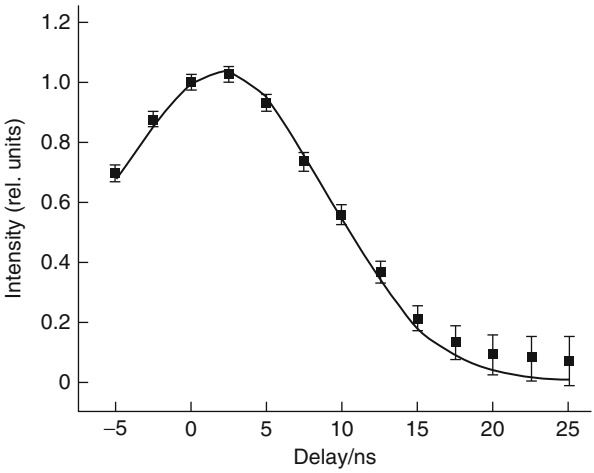

Fig. 30.7 Fluorescence kinetic curve of tryptophan excited by a 10-ns laser pulse with $F < 10^{23}$ cm^{2}s^{-1}; *squares* are experimental data, the *solid curve* is the theoretical dependence

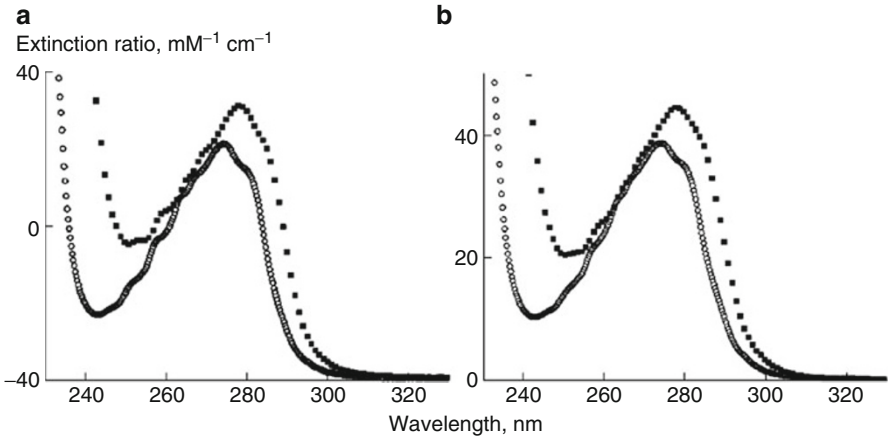

Fig. 30.8 Absorption spectra of (**a**) HSA (*squares*) and an equimolar solution of tryptophan, tyrosine, and phenylalanine (1:18:31) (*circles*) and (**b**) BSA (*squares*) and an equimolar solution of tryptophan, tyrosine, and phenylalanine (2:20:27) (*circles*)

However, information obtained using conventional methods of fluorescence spectroscopy is often insufficient for the interpretation of the structural organization of proteins and use as the descriptors of living systems. The analysis can be significantly improved by using laser methods (such as nonlinear, kinetic, and, especially, "matrix" laser fluorometry), which, in addition to traditional fluorescent parameters describing the shape and position of fluorescence bands, allows one to determine the molecular photophysical parameters of fluorophores (such as the lifetime, absorption cross section, rate of energy transfer, etc.) under a lack of a priori information necessary for conventional methods (see Sect. 30.2). These parameters can be used as diagnostic identifiers.

In Ref. [13], an approach based on the use of the nonlinear laser fluorometry method that allows one to determine in the experiment the individual photophysical parameters of fluorophores in single-tryptophan-containing (using the example of human serum albumin) and two-tryptophan-containing (using the example of bovine serum albumin) proteins is suggested and developed. The latter can exhibit the excitation energy transfer between tryptophan residues within one protein macromolecule (intramolecular energy transfer); therefore, the solution of this protein is an example of an ensemble of localized donor–acceptor pairs. Individual photophysical parameters of the mentioned proteins have been determined for the first time. The values of the photophysical parameters received for concrete objects (albumins) can be used for the diagnostics of biological systems containing these proteins.

Serum albumins are globular proteins accomplishing the transport function in blood plasma. The structure and biological functions of albumins can be found in Ref. [34]. Tryptophan, tyrosine, and phenylalanine (with relative contents of 1:18:31 in HSA and 2:20:27 in BSA [34]) are the absorption groups (chromophores) in proteins, including albumins. The tyrosine fluorescence in HSA and BSA (as in many other natural proteins) is quenched due to the effect of adjacent peptide bonds, polar groups (such as CO, NH_2), and other factors [26], and phenylalanine has a low fluorescence quantum yield [26]. Therefore, the fluorescence signal in these proteins is determined mainly by tryptophan residues. As described in Ref. [34], HSA and BSA have a similar amino acid sequence and spatial structure. However, HSA contains one tryptophan residue in the protein matrix (Trp214), and BSA contains two residues (Trp212 and Trp134). Trp212 in BSA and Trp214 in HSA have a similar microenvironment and, hence, their spectral properties are similar [35]. Tryptophans of BSA are not spectrally identical due to the stronger integration of Trp212 into the protein's structure and the more hydrophobic environment of Trp212 in comparison with Trp134 [35]. The distance between tryptophans in BSA is about 3.5 nm [34]. This fact makes the intramolecular energy transfer between them using the Forster resonance energy transfer (FRET [6]) mechanism possible.

The absorption spectra of the objects under study and (for comparison) the corresponding equimolar solutions (solution of tryptophan, tyrosine, and phenylalanine at the same ratio as they are contained in protein) are shown in Fig. 30.8. It is seen that the parameters of the absorption bands of proteins do not coincide with the corresponding parameters for the equimolar solutions.

The fluorescence spectra of the proteins and the solution of the free tryptophan (the tryptophan in a water solution was investigated in Ref. [13]) are presented in Fig. 30.9. One can see that the fluorescence of the proteins is blue shifted relative to the tryptophan fluorescence (353 nm) in a buffer solution. This is due to a decrease in the tryptophan environment polarity in the proteins. The maximum of the HSA fluorescence (332 nm) is blue shifted in comparison with BSA (342 nm). Because the fluorescence spectrum of the tryptophan residues reflects the polarity of their nearest environment, and since the properties of the environments of Trp212 in BSA and Trp214 in HSA are similar [35], such a shift can be related to the fact that

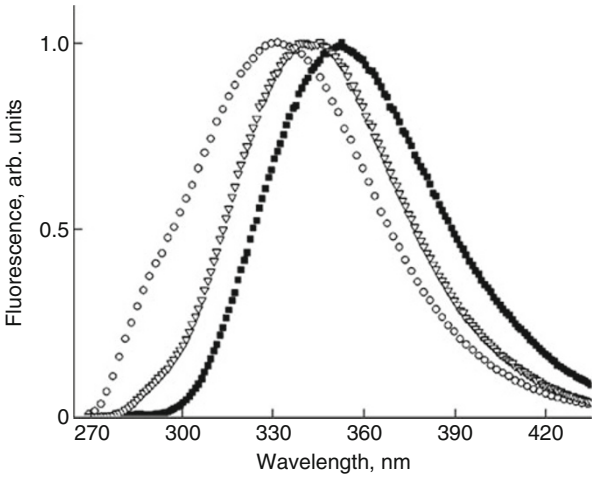

Fig. 30.9 Fluorescence spectra of HSA (*circles*), BSA (*triangles*), and tryptophan (*squares*) in a phosphate buffer with a concentration of 10^{-5} M

BSA contains tryptophan Trp134 located in the environment with a higher polarity (in comparison with Trp212). Thus, the total fluorescence spectrum of BSA is red shifted.

In Ref. [13], application of NLF in complex with time-resolved fluorometry to diluted solutions of HSA and BSA yielded new information about their photophysical characteristics. The results of the investigation performed are presented below.

In this work, solutions of human serum albumin (HSA) (>96 %, Sigma) and of bovine serum albumin (BSA) (>98 %, MP Biomedicals) in a phosphate buffer (0.01 M, pH 7.4) were used. The concentrations were 10^{-5} (during the measurement of the absorption spectra and the fluorescence spectra at spectrofluorometer) and 10^{-9} M (during the measurement of the fluorescence spectra, kinetic curves, and nonlinear curves at the laser fluorometer). All of the experiments were performed at a temperature of 25 °C ± 1 °C.

Fluorescence saturation curves and fluorescence kinetics were measured with the use of a spectrometer described in Sect. 30.3.2. Experimental data were processed using the models of fluorescence response given in Sect. 30.2.

The fluorescence bands at several values of photon flux density F of the exciting laser radiation are shown in Fig. 30.10. One can see that the maximum of the HSA fluorescence band does not change its position when F is changed. This is due to the fact that HSA contains one saturating fluorophore. However, the BSA fluorescence band is blue shifted (from 340 to 335 nm) when F is increased, owing to the fact that BSA contains two fluorophores in different environments (therefore, with different spectral properties), which exhibit different degrees (factors) of saturation. Taking into account the blue shift of the HSA fluorescence spectrum (in comparison with the BSA fluorescence spectrum) and the similarity of the properties of Trp214 in HSA and Trp212 in BSA, one can assume that, in the system of two tryptophans of BSA, Trp212 serves as the donor of the energy, and Trp314 is the acceptor (i.e., its fluorescence spectrum is presumably shifted towards long wavelengths).

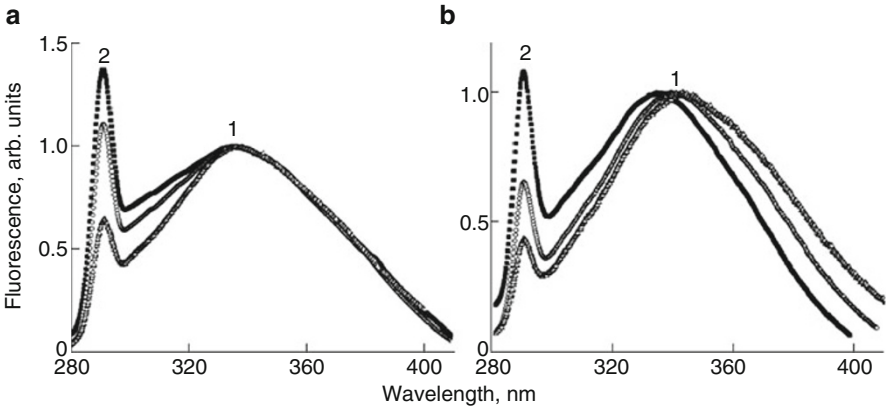

Fig. 30.10 Fluorescence bands (*1*) of proteins HSA (**a**) and BSA (**b**) and Raman scattering from water molecules (*2*) at several values of photon flux density (*F*). The band with a maximum value of F ($F = 4 \cdot 10^{25}$ cm^{-2} s^{-1}) corresponds to the maximum value of the Raman scattering from water molecules

The kinetic curves and the fluorescence saturation curves of BSA are shown in Fig. 30.11. For BSA, the saturation curves depend on the registration wavelength in the wavelength range 310–390 nm. This is due to the fact that the BSA fluorescence band is a superposition of the bands of two tryptophans possessing different spectral properties. A similar difference in the curves for HSA is negligible.

For the determination of the photophysical parameters of HSA fluorophore, the inverse problems of nonlinear fluorometry were solved with the model, described by (30.8) and (30.9) (see Sect. 30.2). For the determination of the individual photophysical parameters of fluorophores of BSA, the inverse problems of nonlinear and kinetic fluorometry were also solved, but, in this case, the model described by (30.11) and Eqs. (30.12) and (30.13) was used; the fluorescence signal was measured at 310 nm (when the kinetic curves and the fluorescence saturation curves for the donor were constructed) and 390 nm (when similar curves were constructed for the acceptor). The resulting values of the parameters of protein fluorophores are presented in Table 30.2.

As one can see from Table 30.2, the values of photophysical parameters σ and τ_3 of Trp214 in HSA and Trp212 in BSA are similar. This result should have been expected based on a comparison of the structures of these proteins. The rates of energy transfer in BSA from excited donor to unexcited acceptor (K_{DA}) and to excited acceptor (K_{SS}) are small in comparison with the rate of intramolecular relaxation (τ_3^{-1}). This can be due to the following reasons: (A) In BSA, the tryptophan residues in the D–A pair are located at a distance that is insufficient for a noticeable energy transfer between them. According to the data on the BSA structure [34], the distance between two tryptophans in the molecule is about 3.5 nm. For comparison, the Forster radius for the energy transfer between free tryptophans ranges from 0.6 to 1.2 nm [26] (depending on the solvent). (B) Perhaps, the mutual orientation of the transition dipoles of fluorophores impedes the energy transfer [6].

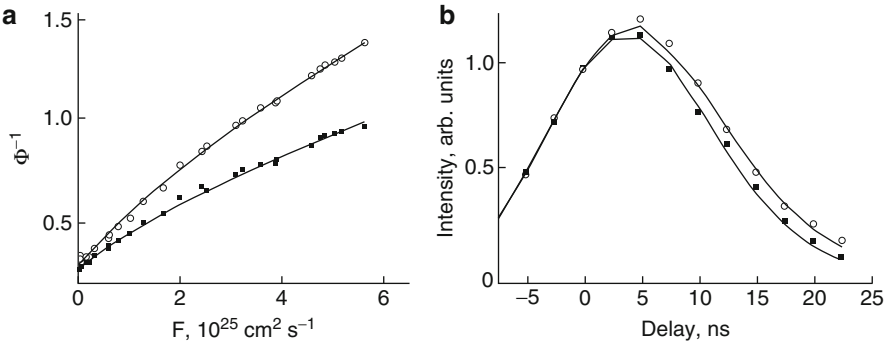

Fig. 30.11 (**a**) Saturation and (**b**) kinetic curves for BSA (registration wavelengths at 390 (*squares*) and 310 nm (*circles*)). *Lines* are plotted using model (30.11) and (Eqs. 30.12) and (30.13) for the parameters presented in the Table 30.2

Table 30.2 Photophysical parameters of fluorophores (tryptophan residues) in human serum albumin (HSA) and bovine serum albumin (BSA)

Protein	Parameters	Tryptophan residues	
HSA		Trp214	
	τ_3, ns	4.5	
	σ,10^{-17} cm^2	1.3	
	K_{32}, s^{-1}	$<10^7$	
BSA		Trp134	Trp212
	τ_3, ns	6.2	5
	σ, 10^{-17} cm^2	3	1
	K_{DA}, s^{-1}	$<10^7$	
	K_{SS}, s^{-1}	$<10^7$	

It is significant that the values of the absorption cross section determined using the method of nonlinear fluorometry are true values for fluorophores and they are obtained without a priori information about the contribution of other groups into absorption at a specific wavelength and about the concentration of fluorophores. This is a unique feature of nonlinear fluorometry. In the literature (see, e.g., Ref. [36]), the absorption cross section of the tryptophan residue in protein is assumed to be equal to the absorption cross section of free tryptophan in solution, because it is supposed that this parameter is weakly dependent on the environment.

However, it is clear that such an assumption is only an estimate. A comparison of the equimolar solution and protein solution absorption spectra (Fig. 30.8) shows that these spectra do not coincide. The absorption cross section for tryptophan in solution is equal to $1.6 \cdot 10^{-17}$ cm^2 [26] (at 266 nm in an aqueous solution); now, it can be compared with the true values of the absorption cross section of tryptophan residues in native proteins (see Table 30.2), which were determined for the first time in Ref. [13].

Nonlinear fluorometry provides a unique possibility to determine one more parameter; namely, the energy transfer rate in a localized D–A pair, in which the measurement of the donors' lifetime in the absence of an acceptor (which is necessary information for the application of a traditional method [6]) is impossible. In BSA as a representative of a macromolecule with a localized donor–acceptor pair, the values of the interfluorophore energy transfer rates *K*DA and *K*SS was 1–2 orders of magnitude lower than the value of the intrafluorophore energy transfer rate; with the use of the suggested method, it became possible to give the upper estimate these values: $K_{DA}, K_{SS} < 10^7\ s^{-1}$.

30.3.4 Nonlinear Laser Fluorometry of Red Fluorescent Protein mRFP1

Fluorescent proteins (FP) are a special class of proteins that have a distinguishing property to form inner fluorescent (and/or absorbing), in a visible wavelength range, center (heterogroup) without involvement of any additional cofactors and ferments (autocatalytic reaction), except for molecular oxygen [37–39]. That center is called a chromophore, even in the case when it produces fluorescence, i.e., it is a fluorophore (as in FP mRFP1). The interest in FPs is determined by several factors: (a) the possibilities to use them as indicators of processes in living cells [37–39]; (b) the structure features [38, 39]; (c) the features of photophysical processes in FPs, which make it possible to use them as model systems with LDA pairs [40, 41].

According to the investigations of the mRFP1 three-dimensional structure [42], there is a tryptophan (tryptophan residue) at the distance of 15 Å from the protein chromophore, which could be a potential partner (the donor of energy) for inductive resonance energy transfer (FRET) to the protein chromophore. It is known [43–47] that the water solution of mRFP1 (and the water solutions of mRFP1 homologs) is a mixture of two or three (it depends on external factors) chemically nonidentical types of molecules (spectral forms). In the literature these forms are called the B, G, and R form of a protein and they have a difference only in chemical structure of the protein chromophore [43, 45–47]. Thereby, one can say that mRFP1 molecule contains a LDA pair and an ensemble of molecules of the protein is a multicomponent ensemble of such pairs.

It is known [43–47] that the balance between B and G forms of FP can be disturbed with a change of the solution acidity (pH indicator) or as a result of light (from the UV, blue, or green spectral range) influence on the protein. Irradiation of the protein molecules by the light from the green spectral range provokes a conversion of G-form molecules to the molecules of B form; as a result, the protein solution will represent a mixture of only two forms (the sum of two sub-ensembles of molecules containing a LDA pair), namely, B and R. An incremental change of the protein solution pH to 9 leads to nearly total transfer of the B-form molecules to the G-form ones. In [15], these procedures decreased the amount of simultaneously existing forms in the mRFP1 solution and the method of the

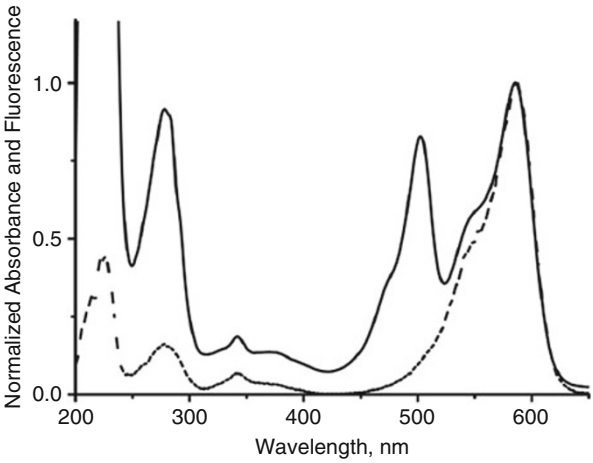

Fig. 30.12 The absorption (*solid curve*) and fluorescence excitation (*dotted curve*, registration wavelength is 607 nm) spectra of mRFP1. The spectra are normalized to the value of the signal intensity at 584 nm

nonlinear fluorometry (combined with kinetic fluorometry) for determining photophysical parameters was used. The experimental setup is described in Sect. 30.3.2. Kinetic curves were obtained with the use of a picosecond fluorometer. Combined use of both methods allows for such a complex object as three-component solution of fluorescent protein (FP) to identify the most relevant set of photophysical parameters that describes the main features of photophysical processes in FP and can be used to diagnose its condition in the environment.

The acceptor fluorescence decay under excitation of an ensemble of donor-acceptor pairs by δ-pulse is described [48] as:

$$I_A(t) = B \times \exp(-t/\tau_A) - A \times \exp(-t/\tau_{D+A}), \tag{30.17}$$

where $B = A + [A^*]_0$, $[A^*]_0$ is the excited acceptor molecules concentration at a time point $t = 0$ (immediately after the excitation pulse is over); $A = [D^*]_0 \times K_{DA}/(1/\tau_{D+A} - 1/\tau_A)$; $[D^*]_0$ is the excited donor molecules concentration at a time point $t = 0$; $\tau_{D+A} = (1/\tau_D + K_{DA})^{-1}$ is the fluorescence lifetime of the donor in the presence of the acceptor; other designations are given above.

The excitation pulse duration and the detector instrument function's width of the spectrometer used in Ref. [15] are an order of magnitude less than the fluorescence lifetimes measured in the experiments. Therefore, after an approximation of the experimental time dependence of object fluorescence intensity by function (30.17), one can determine the lifetimes τ_A, τ_{D+A}, and the partial contributions of B and A components of the fluorescence decay curve.

As has been mentioned, the obtained preparation of the mRFP1 is a mixture of three chemically nonidentical sub-ensembles of molecules (G, B, and R forms of protein). The excitation of the protein solution by irradiation at a wavelength of 270 nm (the absorption maximum of the tryptophan in the protein [49], see Fig. 30.12) leads to appearance in the signal spectrum not only of an UV band (maximum at 330 nm), which corresponds to the tryptophan fluorescence in the

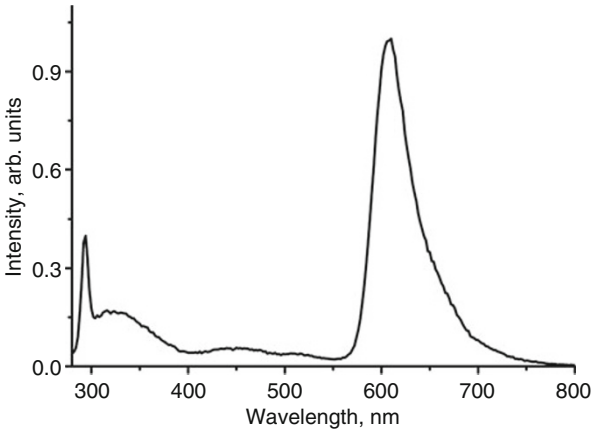

Fig. 30.13 Fluorescence spectrum of mRFP1 under excitation by radiation with the wavelength of 270 nm

protein matrix [49], but also of a band in the visible region of wavelengths (maximum at 607 nm) corresponding to fluorescence of the chromophore mRFP1 R form (Fig. 30.13) [50]. The chromophore of B and G forms of the protein is nonfluorescent [50].

In principle, there are two possible mechanisms of the R-chromophore fluorescence band appearance under UV-light (the wavelength around 270 nm) excitation: (a) direct light absorption by the chromophore; in this case the chromophore is transferred to a higher state than the first excited singlet one, with further nonradiative relaxation to the first excitation level; (b) the energy transfer from tryptophan to the chromophore, through a higher than the first, excited level of the chromophore. By using only absorption, fluorescence excitation, and emission spectra one cannot define the contributions of these two mechanisms.

The method of nonlinear fluorometry allowed in [15] to reveal that, under UV-light irradiation (the wavelength around 270 nm, namely, 266 nm), the predominant mechanism of the fluorescence band (which we mentioned above) – excitation – is the energy transfer from tryptophan. Moreover, using this method one can obtain the value of the energy transfer rate and the values of other significant photophysical parameters. Below we describe the procedure of resolving this task according to Ref. [15].

The processing of the fluorescence decay curve of the mRFP1 using (30.17), which was obtained under picosecond pulsed laser excitation (excitation wavelength is 266 nm) and registered in the range of the R-form chromophore fluorescence (other forms' chromophores are not fluorescent), allowed determination of the lifetime values $\tau_A = 3$ ns and $\tau_{D+A} = 0.24$ ns [15].

The values of pre-exponential coefficients B and A in (30.4) were found to be practically equal. This is indicative of the absence of the direct excitation of the acceptor [48], therefore, in the (30.11), we can assume $\sigma_A = 0$ (under excitation at $\lambda_{ex} = 266$ nm) and for this reason, the acceptor fluorescence (under this wavelength excitation) is a result of the energy transfer from the tryptophan to the chromophore.

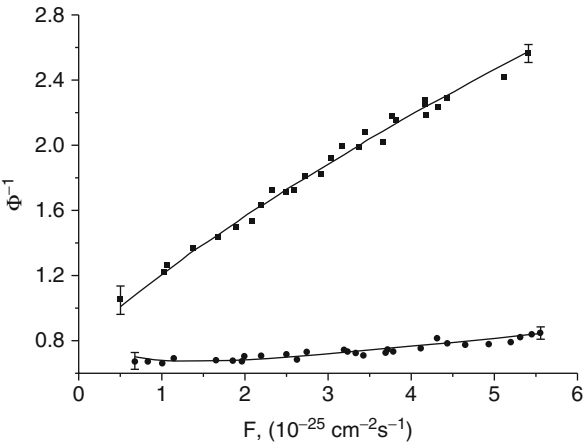

Fig. 30.14 The saturation curves of the donor (*circles*, fluorescence registration at 330 nm) and the acceptor (*squares*, fluorescence registration at 607 nm) in mRFP1 for the mixture of the R and G forms

At the value of pH = 7.4, the mRFP1 solution is represented as a sum of three sub-ensembles of molecules with the LDA pair, each having its own set of photophysical parameters. It is difficult to resolve the inverse task of the nonlinear fluorometry in such a situation, because the number of unknown parameters is too large. But, as we have mentioned above, there are the techniques that allow reducing the number of simultaneously presented forms to two.

In Ref. [15] the following procedure was performed:

(a) The value of the protein solution pH was kept near 9; in this situation, the protein solution contains only protein molecules of R and G forms. After that, two saturation curves were under excitation at the wavelength of 266 nm and registration at 330 nm (the fluorescence saturation curve of the donor, which is determined by the fluorescence signal from tryptophan contained in protein molecules of the R and G forms) and at 607 nm (the fluorescence saturation curve of the acceptor, which is determined by the chromophore fluorescence signal only from the protein molecules of the R-form). Resolving the inverse task of nonlinear fluorometry, in which the fluorescence response formation is described by the model of the collective states of the LDA pair (see Sect. 30.2.5) and the values of the parameters τ_{D+A}, τ_A, $\sigma_A = 0$ for R-form of the protein are considered to be known (see above), the values of K_{DA} (for the R and G forms) and τ_A (for the G form) were determined.

The experimental dependences ${\Phi^{-1}}_D(F)$ and ${\Phi^{-1}}_A(F)$ for case (a) are presented in Fig. 30.14. In order to obtain the saturation curves ${\Phi^{-1}}_D(F)$ and ${\Phi^{-1}}_A(F)$, the first and second orders of RS valence band of water molecules (the wavelengths are 291 and 582 nm, correspondingly) were used as a reference signal; the excitation was at $\lambda_{ex} = 266$ nm.

Having performed this procedure by the use of the model of collective states of the LDA pair, the photophysical parameters (see Table 30.3) were determined. The parameters measured in Ref. [15] by the complex of methods based on the nonlinear fluorometry formed a practically complete set of the parameters that describe the photophysical processes in the molecules of three sub-ensembles of the protein mRFP1, containing a LDA pair.

Table 30.3 The values of the photophysical parameters of the LDA pairs in mRFP1 protein

Parameter[a]	R-form	B-form	G-form
$\sigma_D(\lambda_{ex} = 266)$, cm^2	$(1 \pm 0.2) \times 10^{-16}$		
$\sigma_A(\lambda_{ex} = 266)$, cm^2	0	Not defined	Not defined
K_{DA}	$(3.7 \pm 0.7) \times 10^9$	$(7.8 \pm 1) \times 10^9$	$(2.5 \pm 0.7) \times 10^9$
E	0.89	0.94	0.84
τ_3^A, ns	3 ± 0.15	1.9 ± 0.4	1.7 ± 0.4
τ_3^D, ns	2.1 ± 0.5		

[a]In the table:
$\sigma_D(\lambda_{ex} = 266)$ and $\sigma_A(\lambda_{ex} = 266)$ – the absorption cross section of the donor and the acceptor at the wavelength of 266 nm;
K_{DA} and $E = K_{DA}/(K_{DA} + 1/\tau_3^D)$ – the rate and efficiency of the energy transfer from the excited donor to the unexcited acceptor;
τ_3^D and τ_3^A – the excited state lifetimes of the donor (in the absence of the acceptor) and the acceptor

As the result, it is important to point out that:

(a) The nonlinear fluorometry method makes it possible to determine the true (not distorted by the effect of other sources of light attenuation at a given wavelength) absorption cross section of a fluorescent molecule in the absence of information on the molecule concentration (which is necessary in the traditional methods of absorption spectroscopy). It is interesting to compare the value obtained for tryptophan in the FP mRFP1 with the values of this parameter for tryptophan in an aqueous solution ($\sigma_{266} = 1.6 \times 10^{-17}$ cm^2 [27]), human serum albumin ($\sigma_{266} = 1.3 \times 10^{-17}$ cm^2 [13]), and bovine serum albumin ($\sigma^D{}_{266} = 1 \times 10^{-17}$ cm^2 and $\sigma^A{}_{266} = 3 \times 10^{-17}$ cm^2 [13]).

(b) We emphasize that the lifetime of the excited state of the donor in the absence of the acceptor has been obtained without the removal of the acceptor. For FP mRFP1, this value also has been obtained first in Ref. [15]. For tryptophan in an aqueous solution, $\tau_D = 2.8$ ns [27]; for tryptophan in human serum albumin, $\tau_D = 4.5$ ns [13]; and for tryptophan in bovine serum albumin, $\tau_D = 5$ ns and $\tau_A = 6.2$ ns [13].

(c) The value τ_A for the chromophore of the R form obtained in Ref. [15] coincides within the error with the parameter obtained in Ref. [51] in the direct excitation to the absorption band of the chromophore. Simultaneously, the excited state lifetime values of the chromophores of the B and G form have been obtained (although the chromophores of these forms are nonfluorescent).

(d) The obtained results show that the high volume ($E = 0.89$) of the energy transfer efficiency from the tryptophan to the chromophores in all three forms of the protein is of special scientific and practical interest. This permits employing mRFP1 as a promising fluorescence indicator that makes use of its own inner LDA pair (an alternative is the preparation of such pairs of two proteins [46, 47]). Let us note that the application of the nonlinear fluorometry enabled us to determine this parameter on conditions that the concentration of the acceptor cannot be changed or the acceptor cannot be totally removed

(in conventional methods of the energy transfer rate measurement, this procedure is assumed [48]) without any preparative actions on the protein (in our case, for the native protein).

30.4 Conclusion

The material presented in the chapter covers the fundamentals of nonlinear fluorometry. This method is not widely used in spectroscopy of COC, although it has some unique features. Among them are the following capabilities that can be of interest for spectroscopists:

- The nonlinear fluorometry method makes it possible to determine the true (not distorted by the effect of other sources of light attenuation at a given wavelength) absorption cross section of a fluorescent molecule in the absence of information on the molecule concentration (which is necessary in the traditional methods of absorption spectroscopy).
- The lifetime of the excited state of the donor in the absence of the acceptor has been obtained without the removal of the acceptor.

These possibilities have been illustrated by the example of proteins (including fluorescent proteins) that attract attention as potential fluorescent tags and indicators of state of the cells, where they can be introduced using gene expression. An approach based on NLF that allows one to determine photophysical parameters of fluorophores within a single protein macromolecule has been developed. In the case of red fluorescent protein mRFP1, these fluorophores are a pair consisting of tryptophan residue and the chromophore that fluoresces in the visible area of spectrum.

The approach uses the formalism of the collective states of a LDA pair and was applied to a ternary ensemble (solution) of the red FP mRFP1 for determination of its photophysical parameters. This allowed quantitative investigation of the photophysical processes in FP macromolecules.

It was shown that the basic channel of the chromophore fluorescence excitation in the R form of the protein under UV radiation at a wavelength of 266 nm is the energy transfer from the tryptophan residue. The rate values of energy transfer from the tryptophan residue to the chromophore for each of three forms coexisting in the ensemble of FP mRFP1 and the individual photophysical parameters (the absorption cross sections and excited state lifetimes) have been determined. It was shown that the tryptophan residue and chromophore in each protein form formed a LDA pair with a high efficiency of energy transfer (approximately 90 %), which makes it possible to use the FP mRFP1 as a prospective fluorescent indicator of the states of living systems. Another advantage of this indicator is the fact that the LDA pair is contained directly in the protein molecule and does not need to be constructed artificially. Thereby, using a rather complex object such as the ternary ensemble of the FP mRFP1 molecules, the abilities of the nonlinear fluorometry method (with excitation by 10 ns pulses of laser radiation) were demonstrated. A wide set of the photophysical parameters have been obtained after processing only two experimental dependences: namely, the fluorescence saturation and kinetic curves.

References

1. Y.R. Shen, *The Principles of Nonlinear Optics* (Wiley, New York, 1984)
2. W. Demtröder, *Laser Spectrocopy* (Springer, New York, 1982)
3. D.S. Kliger (ed.), *Ultrasensitive Laser Spectrocopy* (Academic, New York, 1983)
4. J.J. Laserna (ed.), *Modern Techniques in Raman Spectroscopy* (Wiley, New York, 1996)
5. D.N. Klyshko, *Photons and Nonlinear Optics* (Nauka, Moscow, 1980) [translation: Gordon and Breach, New York, 1988]
6. J.R. Lakowicz, *Principles of Fluorescence Spectroscopy*, 2nd edn. (Kluwer/Plenum, New York, 1999)
7. R.M. Measures, *Laser Remout Sensing* (Wiley, New York, 1984)
8. Q. Peng et al., Lasers in medicine. Rep. Prog. Phys. **71**(056701) (2008)
9. V.V. Fadeev, T.A. Dolenko, E.M. Filippova, V.V. Chubarov, Saturation spectroscopy as a method for determining the photophysical parameters of complicated organic compounds. Opt. Commun. **166**, 25–33 (1999)
10. S.A. Dolenko, T.A. Dolenko, V.V. Fadeev, E.M. Filippova, O.V. Kozyreva, I.G. Persiantsev, Solution of inverse problem in nonlinear laser fluorimetry of organic compounds with the use of artificial neural networks. Pattern Recogn. Image Anal. **9**(3), 510–515 (1999)
11. I.V. Boychuk, T.A. Dolenko, A.R. Sabirov, V.V. Fadeev, E.M. Filippova, Study of the uniqueness and stability of the solution of inverse problem in saturation fluorimetry. Quantum Electron. **30**(7), 611–616 (2000)
12. T.S. Gostev, V.V. Fadeev, Determination of photophysical parameters of chlorophyll a in photosynthetic organisms using the method of nonlinear laser fluorimetry. Quantum Electron. **41**(5), 414–419 (2011)
13. A.A. Banishev, E.A. Shirshin, V.V. Fadeev, Laser fluorimetry of proteins containing one and two tryptophan residues. Laser Phys. **18**(7), 861–867 (2008)
14. E.A. Shirshin, A.A. Banishev, V.V. Fadeev, Localized donor-acceptor pairs of fluorophores: determination of the energy transfer rate by nonlinear fluorimetry. JETP Lett. **89**(10), 475–478 (2009)
15. A.A. Banishev, E.A. Shirshin, V.V. Fadeev, Determination of photophysical parameters of red fluorescent protein mRFP1 under ultraviolet excitation by methods of laser fluorimetry. Appl. Opt. **49**(34), 6637–6644 (2010)
16. E.M. Filippova, V.V. Fadeev, V.V. Chubarov, S.M. Glushkov, T.A. Dolenko, Laser fluorescence spectroscopy as a method for studying humic substance. Appl. Spectrosc. Rev. **36**(1), 87–117 (2001)
17. D.V. Maslov, E.E. Ostroumov, V.V. Fadeev, Saturation fluorimetry of complex organic compounds with high local concentration of fluorophores (by the example of phytoplankton). Quantum Electron. **36**(2), 163–168 (2006)
18. V.Z. Pashenko, L.B. Rubin, Laser spectroscopy of the photosynthesis energy conversion. Sov. J. Quantum Electron. **5**(10), 2196–2205 (1978)
19. V.V. Fadeev, T.A. Dolenko, D.V. Il'in, P.N. Litvinov, A.A. Meshkantsov, Matrix method of laser fluorimetry of complex organic compounds in water. EARSeL eProc. **3**(1), 191–196 (2004)
20. V.V. Fadeev, Possibility of standardisation of normalized fluorescent parameters as a measure of organic admixtures concentration in water and atmosphere. Proc. SPIE **3821**, 458–466 (1999)
21. S.A. Dolenko, T.A. Dolenko, V.V. Fadeev, I.V. Gerdova, M. Kompitsas, Time-Resolved Fluorimetry of Two-Fluorophore Organic Systems Using Artificial Neural Networks. Opt. Commun. **213**(4), 309–324 (2002)
22. F. Lewitzka, U. Bunting, P. Karelischek, M. Niederkruger, G. Marowsky, Quantitative analysis of aromatic molecules in water by laser induced fluorescence spectroscopy and multivariate calibration techniques, in *International Conference of "Envirosense" (Europto series)*, Munich, Germany, vol. 3821 (1999), pp. 331–338

23. P. Karlischek, F. Lewitzka, U. Bunting, M. Niederkruger, G. Marowsky, Detection of aromatic pollutants in the environment by using UV-laser-induced fluorescence. Applied Physics B **67**, 497–504 (1998)
24. L. Stryer, Fluorescence energy transfer as a spectroscopic ruler. Annu. Rev. Biochem. **47**, 819–846 (1978)
25. G. Srinivas, A. Yethiraj, B. Bagchi, FRET by FET and dynamics of polymer folding. J. Phys. Chem. B **105**, 2475–2478 (2001)
26. E.A. Permyakov, *Metod sobstvennoi lyuminestsentsii belka (Method of the Intrinsic Protein Luminescence)* (Nauka, Moscow, 2003)
27. A.A. Banishev, E.A. Shirshin, V.V. Fadeev, Determination of photophysical parameters of tryptophan molecules by methods of laser fluorimetry. Quantum Electron. **38**, 77–81 (2008)
28. R.J. Robbins, G.R. Fleming, G.S. Beddard, G.W. Robinson, P.J. Thistlethwaite, G.J. Woolfe, The photophysics of aqueous tryptophan: pH and temperature effects. J. Am. Chem. Soc. **102**, 6271–6277 (1980)
29. D. Bryant, R. Santus, L.I. Grossweiner, Laser flash photolysis of aqueous tryptophan. J. Phys. Chem. **79**(25), 2711–2716 (1975)
30. R. Klein, I. Tatischeff, M. Bazin, R. Santus, Photophysics of Indole. Comparative study of quenching, solvent, and temperature effects by laser flash photolysis and fluorescence. J. Phys. Chem. **85**, 670–677 (1981)
31. P.S. Sherin, O.A. Snytnikova, Y.P. Tsentalovich, Tryptophan photoionization from prefluorescent and fluorescent state. Chem. Phys. Lett. **391**, 44–49 (2004)
32. D. Creed, The photophysics and photochemistry of the near-uv absorbing amino acids-I. Tryptophan and its simple derivatives. Photochem. Photobiol. **39**(4), 537–562 (1984)
33. B. Finstrom, F. Tfibel, L. Lindqvist, One- and two-photon ionization of aqueous tryptophan by the harmonics of the Nd laser. Chem. Phys. Lett. **71**(2), 312–316 (1981)
34. T. Peters Jr, *All About Albumin: Biochemistry, Genetics, and Medical Applications* (Academic, San Diego, 1996)
35. M. Eftink, C.A. Ghiron, Exposure of tryptophanyl residues and protein dynamics. Biochemestry **16**, 5546–5557 (1977)
36. C.N. Pace, F. Vajdos, L. Fee, G. Grimsley, T. Gray, How to measure and predict the molar absorption coefficient of a protein. Protein Sci. **4**, 2411–2423 (1995)
37. R.Y. Tsien, The green fluorescent protein. Annu. Rev. Biochem. **67**, 509–544 (1998)
38. O. Shimomura, *The Discovery of Green Fluorescent Protein* (Wiley, New York, 1998)
39. B.W. Hicks, *Green Fluorescent Protein: Applications and Protocols* (Humana Press, New Jersey, 2002)
40. B. Lounis, J. Deich, F.I. Rosell, S.G. Boxer, W.E. Moerner, Photophysics of DsRed, a red fluorescent protein, from the ensemble to the single-molecule level. J. Phys. Chem. B **105**, 5048–5054 (2001)
41. R. Steinmeyer, A. Noskov, C. Krasel, I. Weber, C. Dees, G.S. Harms, Improved fluorescent proteins for single-molecule research in molecular tracking and co-localization. J. Fluoresc. **15**, 707–721 (2005)
42. D. Yarbrough, R. Wachter, K. Kallio, M. Matz, S. Remington, Refined crystal structure of DsRed, a red fluorescent protein from coral, at 2.0-A resolution. Proc. Natl. Acad. Sci. USA **98**, 462–467 (2001). http://www.rcsb.org/pdb/explore.do?structureId=1G7K
43. V.V. Verkhusha, D.M. Chudakov, N.G. Gurskaya, S. Lukyanov, K.A. Lukyanov, Common pathway for the red chromophore formation in fluorescent proteins and chromoproteins. Chem. Biol. **11**, 845–854 (2004)
44. M. Chattoraj, B.A. King, G.U. Bublitz, S.G. Boxer, Ultra-fast excited state dynamics in green fluorescent protein: multiple states and proton transfer. Proc. Natl. Acad. Sci. USA **93**, 8362–8367 (1996)
45. A.F. Bell, D. Stoner-Ma, R.M. Wachter, P.J. Tonge, Light-driven decarboxylation of wild-type green fluorescent protein. J. Am. Chem. Soc. **125**, 6919–6926 (2003)

46. A.A. Pakhomov, N.Y. Martynova, N.G. Gurskaya, T.A. Balashova, V.I. Martynov, Photoconversion of the chromophore of a fluorescent protein from *Dendronephthya* sp. Biochem. (Moscow) **69**, 901–908 (2004)
47. S. Habuchi, M. Cotlet, T. Gensch, T. Bednarz, S. Haber-Pohlmeier, J. Rozenski, G. Dirix, J. Michiels, J. Vanderleyden, J. Heberle, F.C. Schryver, J. Hofkens, Evidence for the isomerization and decarboxylation in the photoconversion of the red fluorescent protein DsRed. J. Am. Cchem. Soc. **127**(8977–8984) (2005)
48. B. Valeur, Resonance energy transfer and its applications, in *Molecular Fluorescence. Principles and Applications*, ed. by B. Valeur. (Wiley-VCH, Weinheim, 2002), pp. 247–272. http://www.sigmaaldrich.com/catalog/product/sigma/m0566?lang=en&region=RU
49. H. Mizuno, A. Sawano, P. Eli, H. Hama, A. Miyawaki, Red fluorescent protein from discosoma as a fusion tag and a partner for fluorescence resonance energy transfer. Biochemistry **40**, 2502–2510 (2001)
50. R.E. Campbell, O. Tour, A.E. Palmer, P.A. Steinbach, G.S. Baird, D.A. Zacharias, R.Y. Tsien, A monomeric red fluorescent protein. Proc. Natl. Acad. Sci. USA **99**, 7877–7882 (2002)
51. A.A. Banishev, E.P. Vrzheshch, D.V. Dmitrienko, V.L. Drutsa, D.V. Maslov, V.Z. Pashchenko, E.A. Shirshin, P.V. Vrzheshch, V.V. Fadeev, A method for determining the individual optical characteristics of posttranslational fluorescent forms of fluorescent proteins with the use of nonlinear laser fluorimetry. Biofizika **52**, 792–798 (2007)